

30. *Three-Dimensional Distribution of Real Bouguer  
Anomalies from Gravity Values Observed  
at Various Elevations.*

By Yukio HAGIWARA,

Earthquake Research Institute.

(Read June 22, 1965.—Received March 31, 1966.)

Abstract

The value of vertical gradient of gravity obtained by actual direct observations does not generally agree with the standard value. So if reductions are made on observed gravity values by adopting the standard value of gradient, appreciable errors in Bouguer anomaly are liable to result. Only by using the real value of vertical gradient at each respective gravity station, can '*real Bouguer anomaly*' which is different from the customary one '*station Bouguer anomaly*' be calculated. On the basis of the potential theory, the author obtained a mathematical relation existing between the two anomalies—real anomaly and station anomaly—in three-dimensional problems. The two anomalies can be connected through a  $49 \times 49$  square matrix for example, so that the real Bouguer anomaly at the center of the  $7 \times 7$  square on the geoid is included in the solutions of the simultaneous equations of 49 variables. This is an extension of Tsuboi's solution of the corresponding problem for the two-dimensional case.

As an example of actual computations, an application of the method is shown for analysing the gravity field over the Onikobe Caldera and its adjacent area. The maximum difference between the two anomalies reached about 20 mgals on the caldera rim. If a local gravity problem in the mountainous areas is to be studied, the real Bouguer anomaly should be used.

1. Introduction

Gravity anomaly has been customarily calculated by assuming that the vertical gradient of gravity is equal to a standard value, 0.3086 mgal/m say. A free-air correction, amounting to  $0.3086H$  mgals, is therefore added to the gravity value observed at a station of which the elevation is  $H$  in units of meter. Quite a few observations, however,

revealed that the vertical gradient of gravity ranged from 0.27 to 0.33 mgal/m. Sometimes the deviations of the vertical gradient from the normal value were reported even larger. In such cases Bouguer anomalies calculated on the basis of the normal value of the vertical gradient should involve a serious error; for example, if we assume a +0.01 mgal/m deviation, the error of the reduction at a height of 500 m above sea level amounts to +5 mgals which is too large to be ignored in discussing local gravity anomalies.

Kumagai<sup>1)</sup> made use of vertical gradient values actually observed in estimating a Bouguer anomaly on the geoid, which he called "sea-level Bouguer anomaly" discriminating it from "station Bouguer anomaly", the Bouguer anomaly calculated with the normal value of the vertical gradient. A station Bouguer anomaly  $\Delta g_0''$  is defined by the following formula

$$\Delta g_0'' = g + 0.3086 H + \delta g_0' + \delta g_0'' - \gamma_0,$$

where  $g$  is the observed value of gravity,  $\delta g_0'$  terrain correction,  $\delta g_0''$  Bouguer correction and  $\gamma_0$  the standard gravity at a point O on the geoid. Meanwhile the sea-level Bouguer anomaly is given by

$$g + \delta g_0' + \delta g_0'' - \left( \gamma_0 + \frac{\partial \gamma}{\partial H} H \right)$$

where the last term is the standard gravity at a point P right above the point O,  $\partial \gamma / \partial H$  being equal to 0.3086 plus deviation of the vertical gradient of gravity anomaly.

Tsuboi<sup>2)</sup> called the anomaly thus defined "real Bouguer anomaly" instead of "sea-level Bouguer anomaly," because we can obtain the distribution of Bouguer anomaly not only on the sea-level but also on any equipotential surface of the earth provided  $H$  is taken as the distance between the station and the equipotential surface. When we discuss local gravity anomalies in a mountainous area, we might rather adopt a datum level at an adequate altitude, for example, an average elevation of topography.

If we take a level much higher than the average topography detailed features of the anomaly tend to vanish. Contrarily, the anomaly reduced to a lower level would become much too undulatory.

1) N. KUMAGAI and E. ABE, *Sokuchi Gakkaishi (Journal of the Geodetic Society of Japan)*, **2** (1956), 123.

2) C. TSUBOI, *Proc. Japan Acad.*, **41** (1965), 386.

Tsuboi obtained a mathematical relation between station Bouguer anomaly and real one in a two-dimensional case. If the distribution of gravity potential is known on a surface enclosing the mass which causes the gravitation we can calculate the distribution on any other surface on the basis of the potential theory.

The present paper describes a method which is an extension of Tsuboi's method to a three-dimensional case. An IBM 7090 computer program for computing real Bouguer anomaly from data of a gravimetric survey is developed. As an example, real Bouguer anomaly over the Onikobe Caldera and the adjacent area, Tohoku District, Japan<sup>3)</sup> is then obtained. The author will also discuss deviation of vertical gradient of gravity with a particular application to the said areas.

### 2. Two-dimensional Case

A section of a model topography is shown in Fig. 1. Thirteen

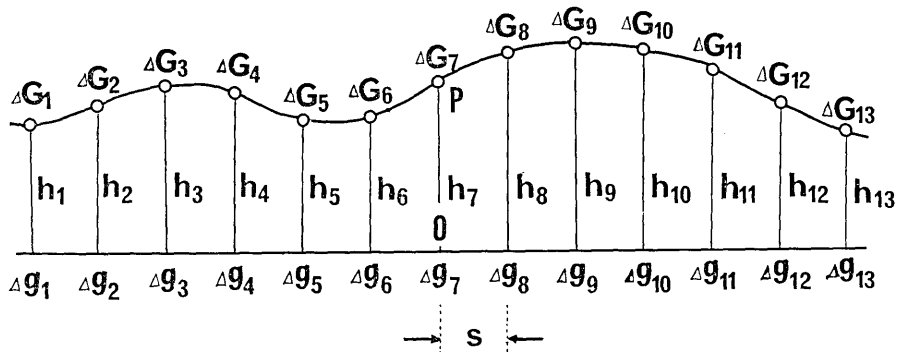


Fig. 1. Section of a model topography.  $\Delta G_i$ : station Bouguer anomaly,  $\Delta g_i$ : real Bouguer anomaly.

gravity stations are arranged with the same intervals in a horizontal direction on the surface of the earth. The station Bouguer anomalies  $\Delta G_i (i=1, 2, \dots, 13)$  at all the stations are assumed to be known by applying customary procedures such as free-air reduction, Bouguer correction and terrain correction to the observed gravity values. The height of each station  $h_i$  is measured in units of  $\pi/3s$ . Our objective is to obtain the real Bouguer anomaly  $\Delta g_7$  at the center point of thirteen stations on the geoid from  $\Delta G_i$  and  $h_i$ . By means of Fourier expansion of  $\Delta g_i$  and potential theory, Tsuboi obtained the following relations bet-

3) T. RIKITAKE et al, *Bull. Earthq. Res. Inst.*, 43 (1965), 241.

ween  $\Delta G_i$  and  $\Delta g_i$ , that is

$$\left. \begin{aligned} \Delta G_4 &= \phi_3(h_4)\Delta g_1 + \phi_2(h_4)\Delta g_2 + \dots + \phi_3(h_4)\Delta g_7 \\ \Delta G_5 &= \phi_3(h_5)\Delta g_2 + \phi_2(h_5)\Delta g_3 + \dots + \phi_3(h_5)\Delta g_8 \\ &\dots\dots\dots \\ \Delta G_{10} &= \phi_3(h_{10})\Delta g_7 + \phi_2(h_{10})\Delta g_8 + \dots + \phi_3(h_{10})\Delta g_{13} \end{aligned} \right\} \quad (1)$$

where

$$\left. \begin{aligned} \phi_0(h_i) &= \frac{1}{6} + \frac{1}{3} \exp(-h_i) + \frac{1}{3} \exp(-2h_i) + \frac{1}{6} \exp(-3h_i) \\ \phi_1(h_i) &= \frac{1}{6} + \frac{1}{6} \exp(-h_i) - \frac{1}{6} \exp(-2h_i) - \frac{1}{6} \exp(-3h_i) \\ \phi_2(h_i) &= \frac{1}{6} - \frac{1}{6} \exp(-h_i) - \frac{1}{6} \exp(-2h_i) + \frac{1}{6} \exp(-3h_i) \\ \phi_3(h_i) &= \frac{1}{12} - \frac{1}{6} \exp(-h_i) + \frac{1}{6} \exp(-2h_i) - \frac{1}{12} \exp(-3h_i) \end{aligned} \right\} \quad (2)$$

Seven simultaneous equations indicated in (1) contain thirteen unknown variables. Since Eq. (1) is hard to solve if the number of variables is too many, it seemed that  $\Delta G_i$  was approximately equal to  $\Delta g_i$  in the case of  $i=1, 2, 3, 11, 12$  and  $13$ , and then these terms were transposed to the left-hand members of (1). Then  $\Delta g_i$  and  $\Delta G_i$  are connected with the  $7 \times 7$  square matrix whose elements are  $\phi_n(h_i)$ 's given by

$$\begin{pmatrix} \Delta G'_4 \\ \Delta G'_5 \\ \Delta G'_6 \\ \Delta G'_7 \\ \Delta G'_8 \\ \Delta G'_9 \\ \Delta G'_{10} \end{pmatrix} = \begin{pmatrix} \phi_0(h_4) & \phi_1(h_4) & \phi_2(h_4) & \phi_3(h_4) & 0 & 0 & 0 \\ \phi_1(h_5) & \phi_0(h_5) & \phi_1(h_5) & \phi_2(h_5) & \phi_3(h_5) & 0 & 0 \\ \phi_2(h_6) & \phi_1(h_6) & \phi_0(h_6) & \phi_1(h_6) & \phi_2(h_6) & \phi_3(h_6) & 0 \\ \phi_3(h_7) & \phi_2(h_7) & \phi_1(h_7) & \phi_0(h_7) & \phi_1(h_7) & \phi_2(h_7) & \phi_3(h_7) \\ 0 & \phi_3(h_8) & \phi_2(h_8) & \phi_1(h_8) & \phi_0(h_8) & \phi_1(h_8) & \phi_2(h_8) \\ 0 & 0 & \phi_3(h_9) & \phi_2(h_9) & \phi_1(h_9) & \phi_0(h_9) & \phi_1(h_9) \\ 0 & 0 & 0 & \phi_3(h_{10}) & \phi_2(h_{10}) & \phi_1(h_{10}) & \phi_0(h_{10}) \end{pmatrix} \begin{pmatrix} \Delta g_4 \\ \Delta g_5 \\ \Delta g_6 \\ \Delta g_7 \\ \Delta g_8 \\ \Delta g_9 \\ \Delta g_{10} \end{pmatrix} \quad (3)$$

where

$$\left. \begin{aligned} \Delta G'_4 &= \Delta G_4 - \phi_3(h_4)\Delta G_1 - \phi_2(h_4)\Delta G_2 - \phi_1(h_4)\Delta G_3 \\ \Delta G'_5 &= \Delta G_5 - \phi_3(h_5)\Delta G_2 - \phi_2(h_5)\Delta G_3 \\ \Delta G'_6 &= \Delta G_6 - \phi_3(h_6)\Delta G_3 \\ \Delta G'_7 &= \Delta G_7 \\ \Delta G'_8 &= \Delta G_8 - \phi_3(h_8)\Delta G_{11} \\ \Delta G'_9 &= \Delta G_9 - \phi_2(h_9)\Delta G_{11} - \phi_3(h_9)\Delta G_{12} \\ \Delta G'_{10} &= \Delta G_{10} - \phi_1(h_{10})\Delta G_{11} - \phi_2(h_{10})\Delta G_{12} - \phi_3(h_{10})\Delta G_{13} \end{aligned} \right\} \quad (4)$$

The real Bouguer anomaly at the point O right under the gravity station No. 7 is calculated with a scalar product of the column vector  $\Delta G'_n$  and the fourth row of the inverse matrix of  $\phi_n(h_i)$ , that is

$$\Delta g_7 = \sum_{n=4}^{10} \varphi_{ln}(h_i) \Delta G'_n, \quad (5)$$

where  $\varphi_{kl}(h_i)$  denotes the  $(k, l)$ th element of the inverse matrix of  $\phi_n(h_i)$ . With a high-speed computer the inverse matrix is easily computed by making use of a "sweep-out method" and so the real Bouguer anomaly can be obtained.

When a more precise computation is needed, a practicable way is to calculate seven real Bouguer anomalies on a plane having the average height of the original thirteen elevations in the first place. The real Bouguer anomaly at the point O on the geoid is then calculated from these seven values. In this case the elements of the square matrix in (3) and (4) can be expressed as  $\phi_n(h_i - \bar{h})$  instead of  $\phi_n(h_i)$ , where  $\bar{h}$  is the average height given by

$$\bar{h} = \frac{1}{13} \sum_{i=1}^{13} h_i. \quad (6)$$

After calculating  $\Delta g_i$ 's ( $i=4, 5, \dots, 10$ ), the seven solutions of the simultaneous equations expressed by (3),  $\Delta g_7^0$ , the real Bouguer anomaly at the point O is obtained as

$$\Delta g_7^0 = \sum_{n=4}^{10} \phi_n(\bar{h}) \Delta g_n. \quad (7)$$

The formula (7) shows the procedure by which we get an anomaly value on the geoid from the anomaly distributed on the surface of the average height. It is evident that a better approximation is achieved by this method.

### 3. Three-dimensional case

For an actual use of real Bouguer anomaly it is highly desirable to develop a method suitable for a three-dimensional problem. In a two-dimensional case topographical elevations and values of station Bouguer anomaly at thirteen points about a point P are, as shown Fig. 1, required for computing the real Bouguer anomaly at the point O on the geoid. When we apply a similar mathematical method to a three-di-

mensional problem, values of elevations and station Bouguer anomaly at 169 grid points have to be prepared for computing the real Bouguer anomaly. Then the square matrix in (3) is written by a major matrix,

$$\Phi = \begin{pmatrix} \Phi_0^4 & \Phi_1^4 & \Phi_2^4 & \Phi_3^4 & 0 & 0 & 0 \\ \Phi_1^5 & \Phi_0^5 & \Phi_1^5 & \Phi_2^5 & \Phi_3^5 & 0 & 0 \\ \Phi_2^6 & \Phi_1^6 & \Phi_0^6 & \Phi_1^6 & \Phi_2^6 & \Phi_3^6 & 0 \\ \Phi_3^7 & \Phi_2^7 & \Phi_1^7 & \Phi_0^7 & \Phi_1^7 & \Phi_2^7 & \Phi_3^7 \\ 0 & \Phi_3^8 & \Phi_2^8 & \Phi_1^8 & \Phi_0^8 & \Phi_1^8 & \Phi_2^8 \\ 0 & 0 & \Phi_3^9 & \Phi_2^9 & \Phi_1^9 & \Phi_0^9 & \Phi_1^9 \\ 0 & 0 & 0 & \Phi_3^{10} & \Phi_2^{10} & \Phi_1^{10} & \Phi_0^{10} \end{pmatrix} \quad (8)$$

where  $\Phi_n^i$  is a minor matrix of  $\Phi$ , and an element of one of the minor matrices is

$$\Phi_n^i = \begin{pmatrix} \phi_{0n}(h_{4i}) & \phi_{1n}(h_{4i}) & \phi_{2n}(h_{4i}) & \phi_{3n}(h_{4i}) & 0 & 0 & 0 \\ \phi_{1n}(h_{5i}) & \phi_{0n}(h_{5i}) & \phi_{1n}(h_{5i}) & \phi_{2n}(h_{5i}) & \phi_{3n}(h_{5i}) & 0 & 0 \\ \phi_{2n}(h_{6i}) & \phi_{1n}(h_{6i}) & \phi_{0n}(h_{6i}) & \phi_{1n}(h_{6i}) & \phi_{2n}(h_{6i}) & \phi_{3n}(h_{6i}) & 0 \\ \phi_{3n}(h_{7i}) & \phi_{2n}(h_{7i}) & \phi_{1n}(h_{7i}) & \phi_{0n}(h_{7i}) & \phi_{1n}(h_{7i}) & \phi_{2n}(h_{7i}) & \phi_{3n}(h_{7i}) \\ 0 & \phi_{3n}(h_{8i}) & \phi_{2n}(h_{8i}) & \phi_{1n}(h_{8i}) & \phi_{0n}(h_{8i}) & \phi_{1n}(h_{8i}) & \phi_{2n}(h_{8i}) \\ 0 & 0 & \phi_{3n}(h_{9i}) & \phi_{2n}(h_{9i}) & \phi_{1n}(h_{9i}) & \phi_{0n}(h_{9i}) & \phi_{1n}(h_{9i}) \\ 0 & 0 & 0 & \phi_{3n}(h_{10i}) & \phi_{2n}(h_{10i}) & \phi_{1n}(h_{10i}) & \phi_{0n}(h_{10i}) \end{pmatrix} \quad (9)$$

Number of the elements of  $\Phi$  amounts to  $49 \times 49$ , while the elements of the right- and left-hand column vectors are expressed as  $\Delta g_{ij}$  and  $\Delta G'_{ij}(i, j=4, 5, \dots, 10)$  respectively.  $\Delta G'_{ij}$  can be denoted with  $\Delta G'_{ij}$ 's and  $\phi_{mn}(h_{ij})$ 's similar to (4).

The values of  $\phi_{mn}(h_{ij})$  is given by an integral formula as follows;

$$\phi_{mn}(h_{ij}) = \int_0^1 \int_0^1 \exp(h_{ij} \sqrt{p^2 + q^2}) \cos mp \cos nq dp dq. \quad (10)$$

As the integral cannot be analytically solved, it is time-consuming to evaluate the integral at various values of  $h_{ij}$ . Fortunately,  $\phi_{mn}(h_{ij})$  could be approximately integrated into the following form as shown by Kanamori<sup>4)</sup>:

4) H. KANAMORI, *Proc. Japan Acad.*, **39** (1963), 469.

$$\begin{aligned} \phi_{mn}(h_{ij}) = & \frac{1}{\{d^2 + (x+y)^2\}\{d^2 + (x-y)^2\}} \left[ e^d d(d^2 - x^2 + y^2) \frac{\sin x}{x} \cos y \right. \\ & + e^d d(d^2 + x^2 - y^2) \cos x \frac{\sin y}{y} - 2d^2 e^d \cos x \cos y \\ & \left. + e^d \{d^2(x^2 + y^2) + (x^2 - y^2)^2\} \frac{\sin x}{x} \frac{\sin y}{y} + 2d^2 \right]. \end{aligned} \quad (11)$$

where  $x = \pm m\pi$ ,  $y = \pm n\pi$  and  $d = h_{ij} - \bar{h}$ .  $\bar{h}$  indicates the mean value of  $h_{ij}$  written as

$$\bar{h} = \frac{1}{169} \sum_{i=1}^{13} \sum_{j=1}^{13} h_{ij}. \quad (12)$$

In an actual computation  $\phi_{mn}(h_{ij})$  is programmed as a function subprogram of the computer. After solving forty-nine variables of the forty-nine simultaneous equations, we get the real Bouguer anomaly distributed on the surface at an altitude of  $\bar{h}$ . Finally,  $\Delta g_{77}^0$ , the real Bouguer anomaly at the point O on the geoid, is obtained by using the summation formula similar to (7), that is

$$\Delta g_{77}^0 = \sum_{m=4}^{10} \sum_{n=4}^{10} \phi_{mn}(\bar{h}) \Delta g_{mn}. \quad (13)$$

In the case mentioned above, gravity stations are situated just at the grid points with the same spacing "s." But in actual gravity surveys the stations are not always coincident with the grid points. It is therefore required to draw contours of station Bouguer anomaly first from the values at the actual gravity stations, and then to read the data for punch cards at the grid points with the same spacing from the contours. The topographical elevations are also read at the same point where anomaly values are read.

#### 4. Actual example

Onikobe area is considered to be a caldera of Krakatau type, with a diameter of about 10 km, which must have been formed by a Neogene volcanic activity. We can see a marked ring structure probably formed by a collapse around the south and west walls of the caldera. A gravimetric survey there was conducted by Rikitake et al.<sup>3)</sup> Seventy-three stations are distributed over an area approximately 20 km × 40 km. The highest gravity station is a triangulation point on Mt. Kamurodake

a peak on the caldera rim, with an altitude of 1261.7 m above sea level, while the top of Mt. Araodake, the central cone, is 984.2 m high. The caldera floor lies at a height of about 300 m. The mean density is estimated to be  $2.27 \text{ g/cm}^3$  for calculation of Bouguer correction and terrain correction. The terrain correction was made by a computer with data of about 5,000 topographical elevations. The map of the station Bouguer anomaly is reproduced in Fig. 2 in which we clearly

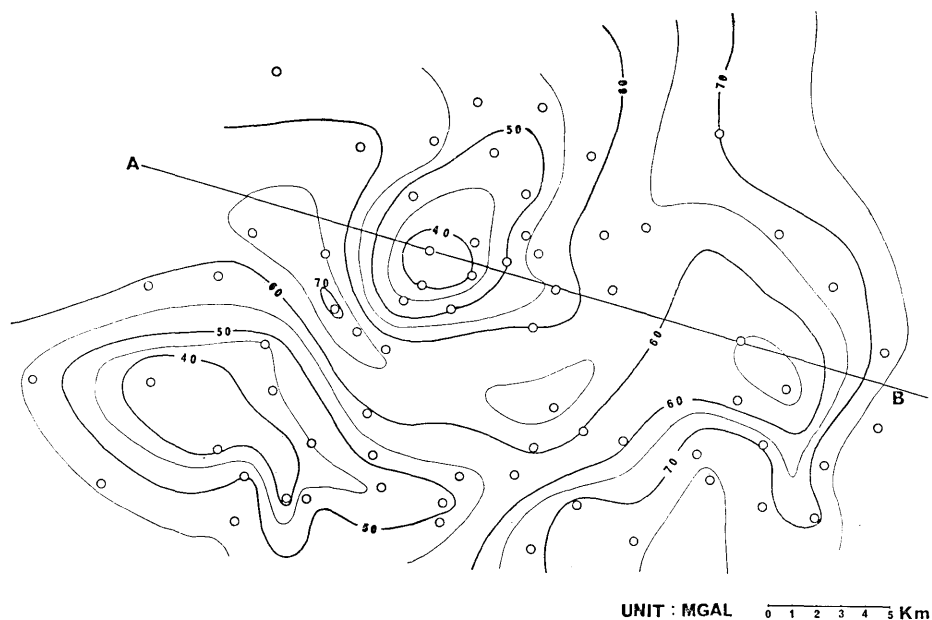


Fig. 2. Map of the station Bouguer anomaly over Onikobe Caldera (after Rikitake et al).

observe three gravity lows; the west one coincides with Maemori-hara Basin, the middle one with the center of the caldera, but we see no geological and topographical evidence for the east one which is covered with a sheet of welded tuff. Along the caldera rim we observe a belt of positive anomaly. Difference in gravity anomaly between the high on the caldera rim and the low on the caldera floor amounts to more than 30 mgals.

Fig. 3 shows the real Bouguer anomaly on the geoid as calculated by the present method. An IBM 7090 computer completed all values of real Bouguer anomaly at a speed of about six seconds per station. We find several conspicuous differences between the station Bouguer anomaly

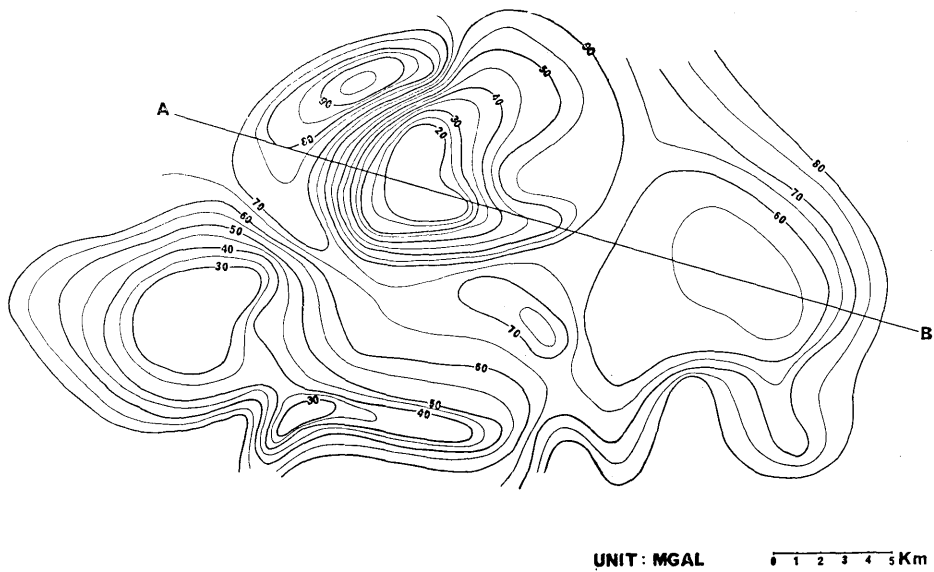


Fig. 3. Map of the real Bouguer anomaly over Onikobe Caldera.

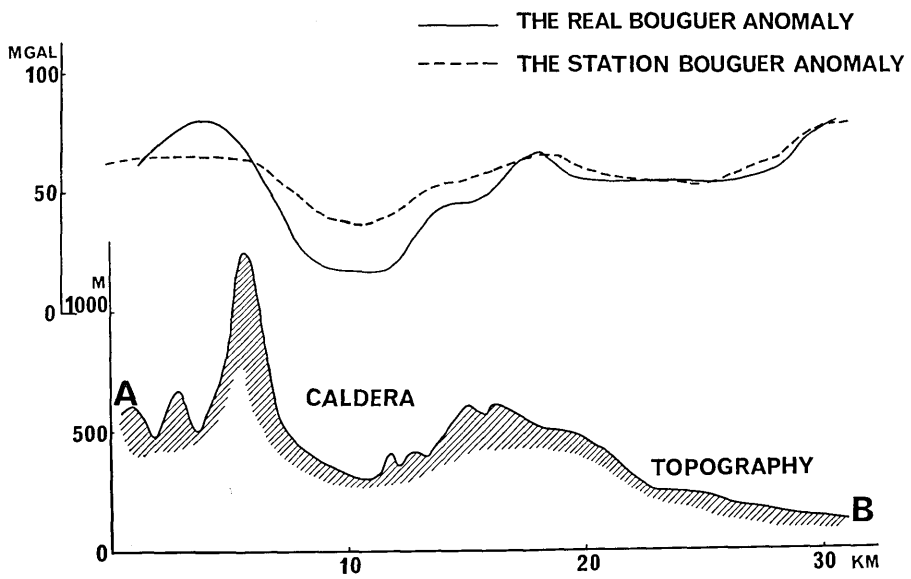


Fig. 4. Gravity profile and topography along the section AB.

and the real one. First, the amplitude of the undulation of the real Bouguer anomaly is larger than that of the station one. An extremely large difference, say 20 mgals, is found at the triangulation point on Mt. Kamurodake. In order to see the differences between them more clearly, a gravity profile along the section AB is shown in Fig. 4. Second, the profile of the station Bouguer anomaly approximately forms a sine wave, while that of the real one looks like a square wave. This fact tells us that waves of shorter length are emphasized in the latter. In other words, a procedure of computing real Bouguer anomaly from station one is equivalent to that transferring an input to an output through a filter whose characteristics have a good gain in high frequency range. However, it is natural that the gain of the filter is identically zero in frequency ranges higher than  $\pi/s$ , where  $s$  denotes the spacing between the grid points. Finally, we find no marked difference between both the anomalies in the eastern part of the profile. The topography there is not steep because of the plateau covered with a thick welded tuff. It is obvious that the real Bouguer anomaly agrees with the station one in relatively flat areas where the effects of terrain correction are negligible. But the difference between the two becomes very important in the case of a local gravity survey over mountainous regions.

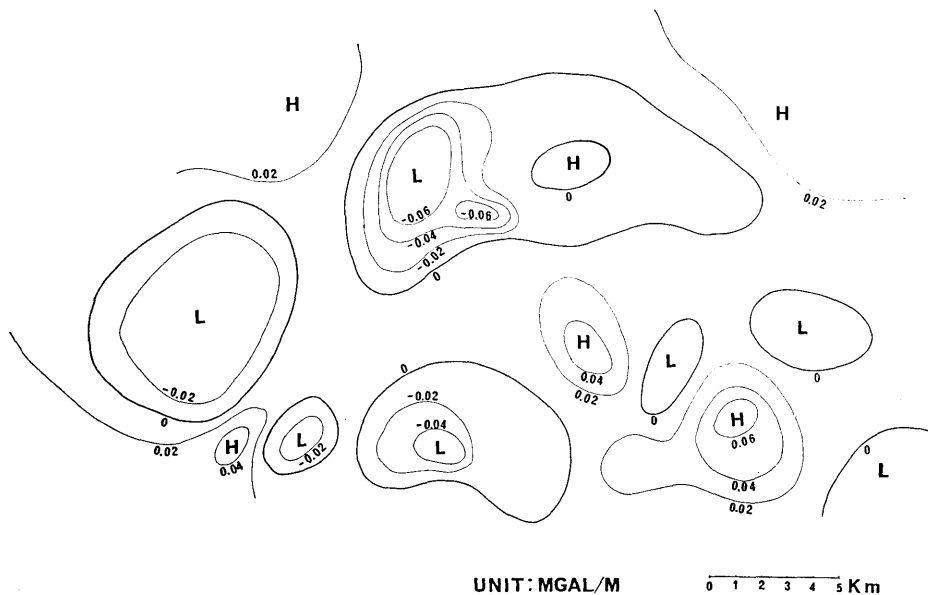


Fig. 5. Deviations of the vertical gradients from the normal value.

The vertical gradient of gravity anomaly is given by the following formula;

$$\frac{\partial g_i}{\partial z} = 0.3086 + \frac{\Delta g_i - \Delta G_i}{h_i}$$

where  $h_i$  is measured in units of meter. The last term of the right-hand members is the deviation of the vertical gradient, the actual computation of which is shown in Fig. 5. We can see in Fig. 5 low gradient ranges in the three geological depressions including Onikobe Caldera. It is also noticeable that a number of lows of vertical gradient are being arranged along topographical lows. On the other hand, the heights agree with the mountain ranges, where outcrops of granitic rocks are taking place. To compute  $\partial g/\partial z$  from  $g$  is equal to a filtering procedure by a high-pass filter. It should be pointed out therefore, that seventy-three stations are insufficient for estimating the distribution of  $\partial g/\partial z$  over an area of approximately  $20 \text{ km} \times 40 \text{ km}$ .

### 5. Concluding remarks

The author extended Tsuboi's method of calculating real Bouguer anomaly to a three-dimensional case. As an actual computation, the real Bouguer anomaly over Onikobe Caldera and the adjacent area was calculated. The computation time was about six seconds per gravity station by an IBM 7090 computer. Marked differences between the real Bouguer anomaly and the station Bouguer anomaly can be seen by the following points:

(1) The amplitude of the undulation of the former on the geoid is generally larger than that of the latter. The maximum difference between the two amplitudes reaches 20 mgals on the caldera rim.

(2) The short wavelength which is included in the latter is emphasized in the former. In other words, the real Bouguer anomaly is the response through a filter whose characteristics have a good gain in a high frequency range.

We may also conclude the following:

(3) We can probably say that the computation of the real Bouguer anomaly is needless where the effect of terrain correction is negligible. But it becomes very important in mountainous regions.

(4) When a local gravity problem, for example, a geophysical prospecting for a metal mine, is treated, the real Bouguer anomaly should not be calculated on the geoid but on an equipotential surface

with an adequate altitude.

(5) The deviation from the normal value of the vertical gradient of gravity is easily estimated by dividing the difference between the two Bouguer anomalies by the elevation of the observed station.

The writer greatly acknowledges the advice and suggestions given by Emeritus Prof. C. Tsuboi. Acknowledgment is also due to Prof. T. Rikitake for his general encouragement.

---

### 30. ジオイド上のブーゲー異常と鉛直勾配

地震研究所 萩原幸男

重力の鉛直勾配は  $0.3086 \text{ mgal/m}$  であるとされるが、実測値は必ずしもこれと一致しない。したがつてもしも正しい勾配がわかつていたならば、 $0.3086 \text{ mgal/m}$  を用いて高度補正をしたブーゲー異常とは異なるブーゲー異常をうるに違いない。坪井はこれを「真のブーゲー異常」と名づけ、これと従来のブーゲー異常とを関係づける 2 次元的数式を考案した。筆者はこれを 3 次元的関係に拡張するために改良し、実例として鬼首カルデラの重力異常値を計算した。その結果カルデラ縁の上では、この両異常の差が最大  $20 \text{ mgal}$  にもおよんだ。この事実は山岳地帯での重力測定値よりブーゲー異常を計算する場合に、この種の計算を無視できないことを物語っている。